Title
Global snow drought hot spots and characteristics

Journal
Proceedings of the National Academy of Sciences of the United States of America, 117(33)

ISSN
0027-8424

Authors
Huning, Laurie S
AghaKouchak, Amir

Publication Date
2020-08-18

DOI
10.1073/pnas.1915921117

Peer reviewed

Global snow drought hot spots and characteristics

Laurie S. Huning[a,1] and Amir AghaKouchak[a,b]

[a]Department of Civil and Environmental Engineering, University of California, Irvine, CA 92697; and [b]Department of Earth System Science, University of California, Irvine, CA 92697

Edited by Benjamin D. Santer, Lawrence Livermore National Laboratory, Livermore, CA, and approved June 23, 2020 (received for review September 17, 2019)

Snow plays a fundamental role in global water resources, climate, and biogeochemical processes; however, no global snow drought assessments currently exist. Changes in the duration and intensity of droughts can significantly impact ecosystems, food and water security, agriculture, hydropower, and the socioeconomics of a region. We characterize the duration and intensity of snow droughts (snow water equivalent deficits) worldwide and differences in their distributions over 1980 to 2018. We find that snow droughts became more prevalent, intensified, and lengthened across the western United States (WUS). Eastern Russia, Europe, and the WUS emerged as hot spots for snow droughts, experiencing ∼2, 16, and 28% longer snow drought durations, respectively, in the latter half of 1980 to 2018. In this second half of the record, these regions exhibited a higher probability (relative to the first half of the record) of having a snow drought exceed the average intensity from the first period by 3, 4, and 15%. The Hindu Kush and Central Asia, extratropical Andes, greater Himalayas, and Patagonia, however, experienced decreases (percent changes) in the average snow drought duration (−4, −7, −8, and −16%, respectively). Although we do not attempt to separate natural and human influences with a detailed attribution analysis, we discuss some relevant physical processes (e.g., Arctic amplification and polar vortex movement) that likely contribute to observed changes in snow drought characteristics. We also demonstrate how our framework can facilitate drought monitoring and assessment by examining two snow deficits that posed large socioeconomic challenges in the WUS (2014/2015) and Afghanistan (2017/2018).

snow | drought | climate | water resources | hydrology

The global importance of snow is irrefutable. Snow cools the Earth's surface; supplies freshwater as snowmelt to one-sixth of the world's population (>1 billion people); and influences biogeochemical processes, ecosystems, and climate (1–3). Snow also attracts tourism and sustains recreational activities, including the multibillion dollar/year global ski industry. People rely on snowmelt for a variety of uses including consumption; agriculture; hydropower; and domestic, industrial, and municipal water (1). While mountain snowmelt runoff can support the agricultural industry in areas where snow rarely occurs (e.g., California's Central Valley), snow also directly provides meltwater to croplands after protectively insulating crops like winter wheat from frost and freeze (e.g., in Russia and Ukraine). Since snow plays such a fundamental role in the global economy, a snow drought or deficit in snow water equivalent (SWE; the amount of water obtained if the snowpack melted instantaneously) can have severe regional and global ramifications, influencing both human activities and ecosystems in snow-covered and snow-free areas.

Across the Northern Hemisphere, the annual average snow cover is an estimated 25 million km^2, with a mean maximum extent of nearly 50 million km^2 in January (4). Over the past decades, a number of studies have advanced our understanding of spatiotemporal changes in snow cover extent (e.g., refs. 4–11); however, snow cover observations do not directly provide information about changes in the amount of SWE and the water storage in the snowpack. Despite significant progress in the remote sensing of snow, many challenges remain when estimating the distribution of SWE both in the Northern Hemisphere, where an estimated 98% of the global snow cover occurs (12), as well as globally (13–17).

The seasonal snowpack stores water during the winter and releases it in the spring and summer when the land surface and overlying atmosphere warm. Global environmental change alters the extent and duration of snow cover and the amount and distribution of SWE. There is, however, considerable regional (and nonuniform) variation in the response of snow cover and SWE to the warming global climate (1, 18–22). Over the western United States (WUS), for example, a decline in the 1 April SWE has been observed, altering the timing of snowmelt runoff (18, 23). Europe has experienced decreases in average and maximum snow depth, except in the coldest regions (21). Increases in SWE across the Karakarom and Tien Shan have occurred in Central Asia (22).

Snow droughts remain relatively unexplored compared to other drought types, and few studies have included critically important snow information for drought characterization (24–30). Moreover, a consistent global framework for monitoring snow droughts does not yet exist, which means that the temporal evolution of persistent SWE deficits remains less studied (27). Some studies have distinguished between dry and warm snow droughts (27, 28, 31). The former are precipitation limited (31). Warm snow droughts occur despite above-normal precipitation since warm

Significance

Given the importance of snow to global food, water, and energy security, characterizing snow deficits (snow droughts) in a changing climate has emerged as a critical knowledge gap. We identify snow drought hot spots and determine how drought duration and intensity vary globally. We show that eastern Russia, Europe, and the western United States experienced longer, more intense snow droughts in the second half of the period 1980 to 2018. During this period, droughts became less intense over the Hindu Kush, Himalayas, extratropical Andes, and Patagonia regions. Natural and human-driven factors (e.g., atmospheric circulation patterns, polar vortex movement, and Arctic warming) likely contribute to snow droughts. We urge the community to further investigate the complex physical drivers of snow drought.

Author contributions: L.S.H. and A.A. designed research; L.S.H. performed research; L.S.H. analyzed data; and L.S.H. and A.A. wrote the paper.

The authors declare no competing interest.

This article is a PNAS Direct Submission.

Data deposition: Data supporting the conclusions in this study can be obtained from https://doi.org/10.6084/m9.figshare.c.5055179. Modern-Era Retrospective Analysis for Research and Applications, version 2, data are available from https://gmao.gsfc.nasa.gov/reanalysis/MERRA-2/data_access/. Moderate Resolution Imaging Spectroradiometer (MODIS)/Terra monthly snow cover data are available from https://doi.org/10.5067/MODIS/MOD10CM.006. The Snow Data Assimilation System and Famine Early Warning System Network snow water equivalent information used in *SI Appendix* over the contiguous United States and Afghanistan can be downloaded from https://doi.org/10.7265/N5TB14TC and https://earlywarning.usgs.gov/fews/product/188, respectively.

[1]To whom correspondence may be addressed. Email: lhuning@uci.edu.

This article contains supporting information online at https://www.pnas.org/lookup/suppl/doi:10.1073/pnas.1915921117/-/DCSupplemental.

First published August 3, 2020.

temperatures favor rainfall over snowfall (31). We consider all types of snow droughts here. Previous regional and basin-scale snow drought studies primarily focused on defining droughts using the maximum (or peak) SWE instead of tracking drought evolution throughout a season (27–29). Examples in literature indicate that using the peak SWE as a proxy for the drought condition or "wetness" of the preceding/subsequent months can result in a misdiagnosis of the drought condition during those earlier/later times (27, 29, 32). For example, a pronounced increase in SWE just prior to the time of peak SWE can cause a season that was below average until that point to be diagnosed as above average, normal, or below average, when the peak SWE value is used as a proxy for the entire season (29, 32). Therefore, the use of peak SWE has deficiencies as a metric for characterizing the temporal evolution of snow drought (27). In contrast, our approach allows analysts to monitor the global evolution of snow drought throughout a season using a single dataset. This capability is important for more reliably estimating vulnerabilities and socioeconomic impacts related to agriculture, water resources, and food security.

Our study provides a worldwide snow drought assessment (33) by introducing a multiscale (e.g., 1-mo and 3-mo) standardized drought framework based on SWE information derived from the Modern-Era Retrospective Analysis for Research and Applications, version 2 (MERRA-2) (34) (see *Materials and Methods* for details). Other existing snow-related drought indices include the Standardized Snowmelt and Rain Index (SMRI) (24) and the Surface Water Supply Index (SWSI) (25). While our standardized SWE index (SWEI) (33) directly incorporates SWE information to monitor the amount of SWE on the ground, the SMRI (based on the sum of rainfall and snowmelt) provides an indication of a streamflow (or hydrological) drought using precipitation and temperature inputs (24). The SWSI also directly uses SWE in its generation; however, its basin-specific calculations for monitoring the total surface water storage pose challenges for interbasin comparisons (35, 36). Comparisons of drought conditions between different regions with different climates or snow regimes are similarly difficult with a percent of normal approach (35, 36). The SWEI does not have this drawback.

Using the SWEI, we conduct a global assessment of the snow drought duration and intensity from October 1980 through September 2018 by focusing on comparisons of these variables during the first and second halves of years. We select these two 19-y periods for analysis since the winter snow cover extent across the Northern Hemisphere exhibited an increase in the 2000s and 2010s, while the previous 2 decades experienced a decrease (4). After analyzing snow drought characteristics, we examine two important recent droughts in the WUS (2014/2015) and Afghanistan (2017/2018) to demonstrate how snow drought information can be used for analyzing specific events. We provide a number of example applications using the SWEI, but users can explore other types of statistical methods beyond those presented here depending on their objectives. We discuss and verify our SWEI product with other datasets in *Materials and Methods* and *SI Appendix*, Figs. S1 and S2.

Global Characterization of Drought Duration

We select seven study regions (map in Fig. 1) for a detailed investigation of the changing drought patterns and to identify snow drought hot spots over the last 4 decades. These regions include the WUS, Europe, Hindu Kush and Central Asia (hereafter Hindu Kush), greater Himalayan region (hereafter Himalayas), and eastern Russia in the Northern Hemisphere and the extratropical Andes and Patagonia in the Southern Hemisphere. The selected regions exhibit statistically significant differences in the distribution of wet and dry conditions during winter and early spring months between the first (1980/1981 through 1998/1999) and second (1999/2000 through 2017/2018) halves of years (see *SI Appendix*, Figs. S3 and S4, for more information). Differences in the distribution of SWEI values or other drought characteristics can occur whether a monotonic trend exists or not (*SI Appendix*, Text S1).

We use our framework for snow drought assessment to understand how snow drought durations have changed over the last 38 y (Fig. 1 and *SI Appendix*, Fig. S5). Throughout this study, we utilize the US Drought Monitor D scale (37) classifications to characterize drought or drier than normal conditions (SWEI ≤ -0.5 or D0 to D4; *Materials and Methods*) and apply a W scale to classify wet spells (SWEI ≥ 0.5 or W0 to W4) as shown in *SI Appendix*, Table S1. During 1999/2000 to 2017/2018, the frequency and duration of droughts increased across the WUS, Europe, and eastern Russia (Fig. 1 and *SI Appendix*, Fig. S5), relative to the previous 19-y period. These regions experienced percent changes in the total drought durations of ∼28, 16, and 2% and in the average drought durations of ∼8, 1, and 3% (respectively). In contrast, the Hindu Kush, Himalayas, extratropical Andes, and Patagonia exhibited declines in the frequency of nearly all drought lengths. The percent changes in the average durations across Patagonia, the Himalayas, extratropical Andes, and Hindu Kush were −16, −8, −7, and −4%, respectively.

Global Characterization of Drought Intensity

Next, for each domain we compute the drought intensity or the negative of the regionally integrated SWEI values for all grid boxes classified as D0 to D4 (abnormally dry to exceptional drought). The intensity indicates the strength or severity of drought conditions across a region. During the latter 19 y, more intense droughts became more probable in the WUS and Europe (Fig. 1) as indicated by the red cumulative distribution functions (CDFs) located to the right of the earlier period (blue CDFs) (*SI Appendix*, Fig. S6). We observe this change across all snow drought intensities except in the upper tail of the distributions. In contrast, the distributional changes between the first and second 19-y periods for the Hindu Kush, Himalayas, extratropical Andes, and Patagonia show an increase in the likelihood of weaker intensity droughts (*SI Appendix*, Fig. S6). Eastern Russia (*SI Appendix*, Fig. S6*E*) displayed a mixed signal where the likelihood of lower-intensity droughts increased during the latter 19 y, whereas the likelihood associated with the most severe droughts in this region decreased or remained unchanged. Hereafter, the percentage increases/decreases provide a comparison of the second analysis period to the first one. The probability that the snow drought intensity would exceed the average values from the first period is 3, 4, and 15% higher in eastern Russia, Europe, and the WUS, respectively (Fig. 1). However, there was a lower chance of this exceedance occurring in the Hindu Kush, extratropical Andes, Patagonia, and Himalayas by 3, 13, 15, and 21%, respectively. *SI Appendix*, Fig. S7, presents a CDF constructed with a subset of the months considered in *SI Appendix*, Fig. S6. Based on *SI Appendix*, Fig. S7, we do not conclude that a change in the intensity of the earlier/later season months is the only control on the relationships seen in *SI Appendix*, Fig. S6, and summarized in Fig. 1.

Snow drought information presented here is consistent with some of the spatiotemporal patterns of changes in other climate variables. We briefly explore a few of these relationships below, together with a brief discussion of some of the physical mechanisms involved in snowpack changes. From 1980 to 2015, some parts of Eurasia (extending from Siberia southward toward study regions C and D in Fig. 1) experienced increased snow cover and albedo during autumn and winter, which has been linked to the loss of Arctic sea ice and rapid warming of the Arctic (known as Arctic amplification) (38, 39). During this period, a persistent movement of the polar vortex away from North America and toward Eurasia (most prominently in February) led to a cooling effect across parts of Eurasia (39). There is evidence of a shift in the polar vortex toward Eurasia in the months December through

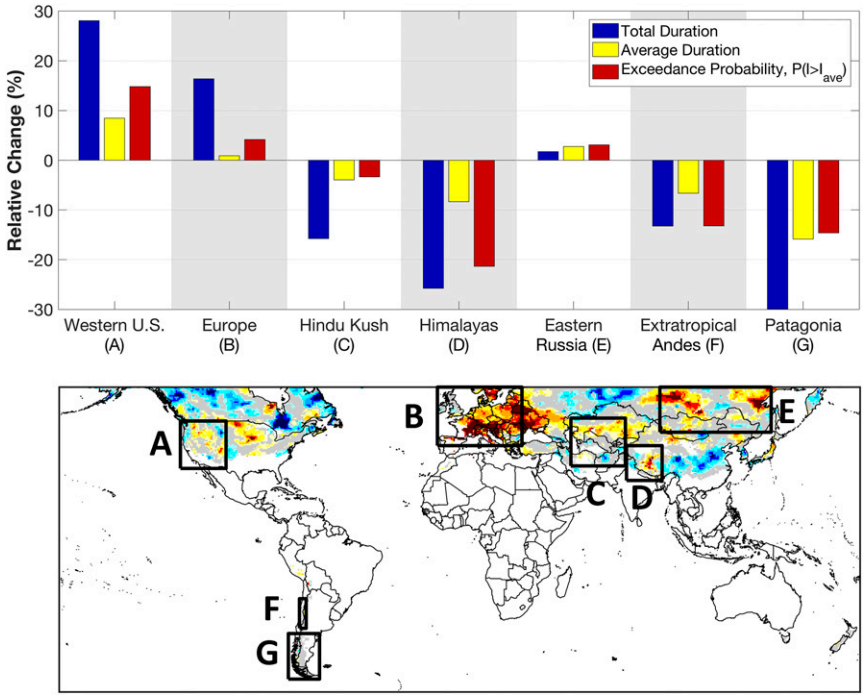

Fig. 1. (*Top*) Relative change in snow drought characteristics around the world from 1980 through 2018. A positive (negative) change indicates that an increase (decrease) in the respective variable occurred during the latter half of years. Percent changes are presented for the total and average durations (difference normalized by the variable value from the first period). The exceedance probability refers to the chance that the drought intensity (I) is greater than the average intensity from the first period (I_{ave}). Changes in probabilities are displayed as differences. (*Bottom*) The sample global SWEI classification map shows the seven study regions (regions A through G).

February, with the largest movement over Eurasia occurring in the 2000s; some component of this shift is presumably related to internal variability (39). The cooling over Eurasia likely contributes to the decrease in the frequency of snow drought conditions over the Hindu Kush and Himalayas.

Cvijanovic et al. (40) suggested that the significant declines in Arctic sea ice extent over recent decades provide a possible connection to precipitation changes over California and certain other midlatitude regions. They described a two-step teleconnection contributing to dry conditions in California when sea ice changes impact tropical convection and cause an anticyclonic response in the North Pacific. Decreasing sea ice extent may have contributed to the increase in snow drought conditions across the WUS and Europe (Fig. 1).

The changes in SWE presented here (and below) likely result from a combination of both natural variability and human-driven factors. We do not attempt to separate these factors by performing a detailed attribution analysis in this study but rather acknowledge that both are contributors to multidecadal changes in SWE. Our results and discussion highlight some of the challenges associated with understanding complex, large-scale phenomena that may influence SWE. They also help frame new possible research directions focusing on the physical drivers and time scales of snow drought. For example, how (and to what extent) do natural and human-related factors amplify or negate each another to influence snow droughts? What common drivers of snow drought (if any) exist across similar geographic (e.g., latitudinal), physiographic (e.g., topographic), or hydroclimatic regions? How do SWE responses to such factors vary both spatially and temporally, impacting society and the environment?

Regional Drought Characteristics and Socioeconomic Impacts

We now characterize two specific events where the snow deficit played a key role in the socioeconomics of a region to show how our framework can be used for drought monitoring and assessment. SWE droughts during the 2013/2014 and 2014/2015 snow seasons had a substantial impact on California and other states in the WUS that derive a large fraction of their water resources from snowmelt (41) (Fig. 2 *A*–*E*). Studies noting the exceptionally low 2014/2015 SWE focused on the peak or 1 April SWE (28, 29, 41–44), which is commonly used to estimate seasonal snowmelt runoff in the WUS. However, in Fig. 2 *A*–*E*, we show the drought as it developed and expanded across time and space in the WUS. The 2014/2015 drought intensified from December to April, with April 2015 being ∼4 times more severe than average (highest intensity in the record). January through April ranked among the top 10 most intense droughts for each of the respective months over the 38 y, with ∼50 to 87% of the snow-covered domain (*Materials and Methods*) exhibiting drought conditions. March 2015 was ∼3 times more intense than on average and ranked second most intense after March 1981 (*SI Appendix*, Fig. S8*C*). Exceptional drought conditions primarily occurred in Washington, Oregon, California, and Nevada in January to March 2015 (Fig. 2 *B*–*D*), whereas they impacted the eastern portion of the WUS (and Nevada) in January and February 1981 before expanding farther west (*SI Appendix*, Fig. S8).

In 2014/2015, California experienced low precipitation and warm temperatures, while Washington and Oregon received near-normal precipitation despite warm temperatures (19, 29, 41–43). Given the snow drought (Fig. 2 *A*–*E*) along with the abovementioned conditions following earlier drought years in California, the state suffered a total economic loss of US$2.74 billion and ∼21,000 jobs in 2015 (45). When the WUS experienced an exceptionally wet winter in 2016/2017, large amounts of SWE and precipitation ended the declared emergency for many of California's counties. Snow droughts developed across portions of the midwestern, northeastern, and southeastern United States, however (Fig. 2 *F*–*I*).

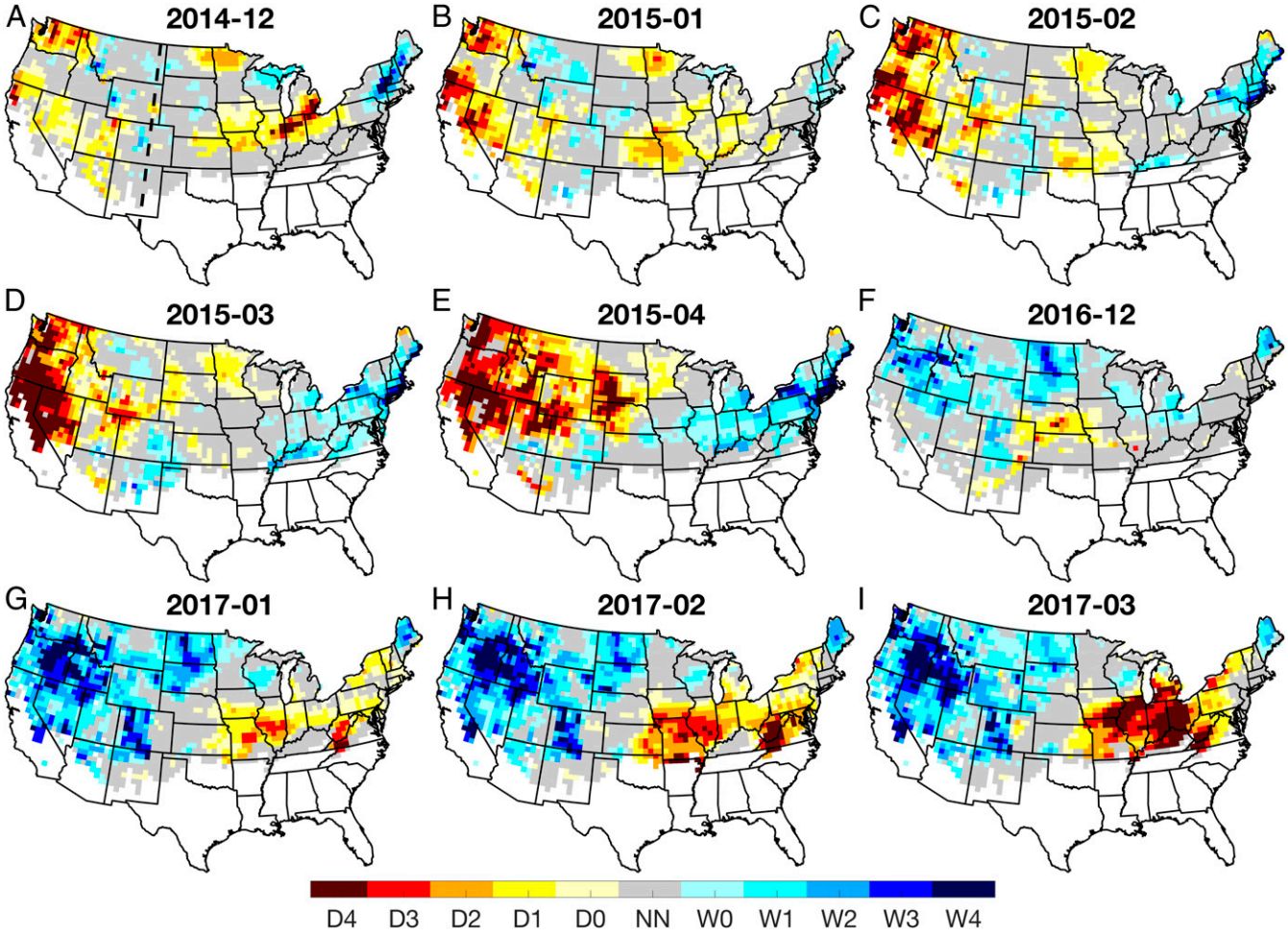

Fig. 2. Three-month SWEI classification for CONUS during (*A–E*) December 2014 to April 2015 and (*F–I*) December 2016 to March 2017. Dashed line in *A* defines the eastern boundary of the WUS (105°W). Classifications used here and hereafter: D0/W0, abnormally dry/wet; D1/W1, moderate drought/wet spell; D2/W2, severe drought/wet spell; D3/W3, extreme drought/wet spell; D4/W4, exceptional drought/wet spell; NN, near normal (*SI Appendix*, Table S1).

A snow drought occurring amid ongoing conflict, violence, and economic challenges can further stress a country like Afghanistan. Afghans rely on snowmelt (e.g., for irrigated croplands), yet have few dams to store runoff from snowmelt (46), leaving the country susceptible to droughts and floods. Years with low SWE cause unexpected humanitarian crises (46). An Afghan proverb even emphasizes the importance of snow: "may Kabul be without gold rather than snow."

During December 2017-March 2018, a widespread snow drought (Fig. 3) encompassed approximately three-fourths or more of Afghanistan's snow-covered domain. Afghanistan experienced record high snow drought intensities in January, February, and March 2018 (3.9 to 4.5 times more severe than average). Among other factors, SWE deficits following previous drought years negatively affected the spring/summer 2018 agricultural season. Food shortages, crop failures, livestock losses, and dry wells and rivers necessitated massive humanitarian efforts for 266,000 drought-affected internally displaced people in 2018 (47). This event also contributed to the food insecurity of ~10.6 million people (~50% of its rural population) in November 2018 (48). The severe linkages between drought (or climatic extremes) and socioeconomic hardships have been discussed before, as in the case of the 2011 Syrian uprising (49) and the collapse of the Mayan civilization (50).

Discussion

We present a general framework for analyzing global snow drought (and wet spell) conditions. Insight into the evolution of snow drought conditions should lead to more informed water management/planning, agricultural practices, and hydropower operations throughout the year. We describe limitations of our study in *Materials and Methods*.

Changes in snow drought characteristics can have ramifications across a number of sectors (water resources, agriculture, tourism, economics, etc.). For example, water managers must balance flood control and storage to meet water demands. In terms of water resources, drought that occurs early in the season may be easier to recover from if above-normal SWE occurs later in the winter or rainfall or glacier melt compensate for the decreased SWE. Despite these compensating factors, the timing and distribution of runoff will likely be altered, which also poses challenges for hydropower operations. Long-term dependence on glacier melt is unsustainable where glaciers experience a continued net loss of mass (51). Early snow drought can contribute to winterkill when winter crops remain unprotected from frost. Having too little SWE can also lead to insufficient agricultural water later in the growing season. A drought occurring later in the season might mean that water managers could have stored more water earlier in the season but may not have in anticipation of runoff from additional late snow accumulation.

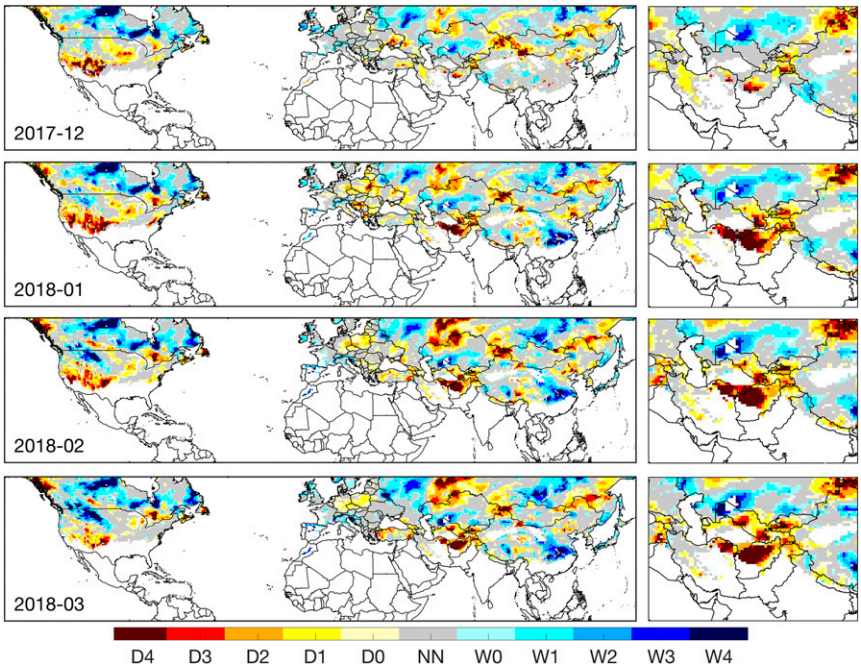

Fig. 3. Three-month SWEI classification during the December 2017 to March 2018 snow drought in Afghanistan: (*Left*) Northern Hemisphere and (*Right*) Afghanistan and surrounding area.

While we focus on low SWE and its ramifications herein, the flexibility of our framework facilitates the examination of periods of extreme SWE accumulation (blue shading in Figs. 2 and 3 and *SI Appendix*, Figs. S8 and S9). This capability is critical because exceptionally snowy and cold periods can disrupt and damage transportation and communication systems, lead to flooding, and cause loss of life. For example, the winter 2009/2010 and 2015/2016 dzuds [periods of heavy snow and cold temperature (52)] across Mongolia (*SI Appendix*, Fig. S9) exacerbated the difficult summer droughts by preventing the already undernourished livestock from grazing in the winter. The former dzud led to the loss of 10 million livestock (52), and the latter threatened 965,000 people (53), contributing to food insecurity, poverty, and human migration to urban areas. Snow droughts and wet spells can have severe socioeconomic impacts across both affluent and developing countries, rural and urban centers, and regions experiencing social unrest and poverty.

Extreme (low or high) SWE events can stress communities, particularly where infrastructure is aging, underdeveloped, and/or inadequate for rapid population growth. When populations are displaced by climatic extremes and social unrest, the competition for resources increases in growing population centers, contributing to anthropogenic drought (human-induced/heightened water stress). Therefore, critical infrastructure (e.g., irrigation, water resources, transportation, and communication systems) must be reassessed and updated to ensure the well-being, water security, and food security of people facing persistent changes or extreme fluctuations in SWE. Changing snow cover can also alter the likelihood of wildfires and impact sediment loading in runoff that affects infrastructure, riparian regions, etc. (3, 19, 54).

The framework introduced here can be used for a wide range of applications including drought monitoring and improving our understanding of the physical drivers of snow drought. It provides an opportunity to obtain additional information on wet/dry cycling, drought severity, and SWE persistence in snowy regions having few (if any) ground-based in situ SWE observations. It also complements other drought frameworks for meteorological, hydrological, and agricultural variables so that appropriate mitigation measures can more effectively be enacted in susceptible sectors worldwide. For example, our approach may be applied to better understand connections between the changing snowpack and risks to agriculture in regions that may need to rely more on alternative sources of water (e.g., cross-basin transfers and additional groundwater pumping) and develop adaptation strategies under snow drought conditions. Examinations of such linkages are important as they can pose food security issues for many people around the world (55).

Materials and Methods

Global Snow Data and Domain. We use SWE from MERRA-2 (34) during October 1980 through September 2018. This global reanalysis has a spatial resolution of 0.5° × 0.625°. Previous studies have shown that MERRA-2 SWE and snow cover estimates are biased relative to observations (56); however, they suggest that MERRA-2's biases may be smaller than other global SWE products particularly across North America (57, 58). We acknowledge large data uncertainties in regions such as high mountain Asia (stretching from the Hindu Kush and Tien Shan in the west to the eastern Himalaya), where SWE information is largely missing. Despite this, our standardized snow drought framework (presented below) depends on the individual ranks of the data values—i.e., it depends on their relative relationship to one another instead of their exact magnitudes. Below and in *SI Appendix*, we also further discuss the ability of our approach to represent periods of drought and surfeit relative to the Snow Data Assimilation System (SNODAS) (59, 60) and Famine Early Warning System Network (FEWS NET) (61).

We combine the MERRA-2 snow information with the level-3 Moderate Resolution Imaging Spectroradiometer (MODIS)/Terra monthly (0.05° resolution) snow cover (SC) product [MOD10CM (62)] to define the global study domain. The monthly SC averages are computed from the corresponding observations in the MODIS MOD10C1 daily maximum snow cover extent observations. The data are generated from the Normalized Difference Snow Index snow cover that leverages the high reflectance of snow in the visible bands and its low reflectance in the shortwave infrared wavelengths. Using the monthly SC from March 2000 through September 2018 (regridded onto the MERRA-2 grid), we compute 3-mo (average) SC climatologies. We select 3 mo here since it matches the time scale in our snow drought analysis described below. We uniformly apply a 5% SC threshold to define the study domain, but further refinement with the MERRA-2 data is required to produce the global snow-covered study domain (see map in Fig. 1). Use of

MODIS SC is advantageous since it provides a satellite-based independent and consistent source of information for defining the global study domain when comparing SWE conditions between MERRA-2 and another dataset (as discussed below and in *SI Appendix*). Relative to the MODIS SC observations, Reichle et al. (56) found that MERRA-2 has a probability of correctly detecting snow cover of 0.86 and a probability of false detection (63) of 0.012, on average.

Using the global domain defined with the SC threshold, we exclude MERRA-2 grid boxes with combined land and land ice fractions below 50%. Furthermore, we only consider grid boxes where at least 75% of a given month (e.g., January) for all years has a nonzero (3-mo) SWE value. For a grid box to be included in the study domain (colored regions in the map in Fig. 1), it must meet these criteria for at least one set of 3 mo (e.g., November–December–January, December–January–February, etc.). We exclude areas poleward of ±60° latitude since SC is not available during polar night (given its use of visible frequencies). An additional constraint is that precipitation poleward of ±62.5° latitude is modeled by MERRA-2 (34).

Standardized Snow Water Equivalent Index. We extend the nonparametric approach described by Farahmand and AghaKouchak (64) to standardize a variable, in this case SWE, for drought monitoring. Since SWE has both zero and nonzero values, we randomly perturb values of zero with positive numbers that are smaller than the lowest nonzero data value. The perturbation only occurs for grid boxes meeting the criteria described above. Rather than fitting a specific distribution function to the data, we determine the probabilities associated with the data by computing the empirical Gringorten (65) plotting position:

$$p(A_{m,i}) = (i - 0.44)/(N + 0.12), \quad [1]$$

where i is the rank of the nonzero variable (from smallest to largest) and N is the sample size. The ranks are determined using the 3-mo integration of SWE for month m, given by

$$A_{m,i} = \mathrm{SWE}_{m-2} + \mathrm{SWE}_{m-1} + \mathrm{SWE}_{m}, \quad [2]$$

where SWE_m is the integrated SWE value for month m derived from MERRA-2. We integrate daily SWE values to derive each of the terms on the right-hand side of Eq. **2**. Therefore, $A_{m,i}$ provides an integrated measure of both the SWE amount and its persistence over each set of 3 mo, which is then standardized as described below. Our approach is analogous to the computation of a 3-mo standardized precipitation index or soil moisture index (64, 66).

We compute the nonparametric standardized SWEI by transforming the empirical probability, p, to the standard normal distribution as follows:

$$\mathrm{SWEI}(A_{m,i}) = \phi^{-1}[p(A_{m,i})], \quad [3]$$

where ϕ^{-1} is the inverse standard normal distribution.

For locations that satisfy the abovementioned criteria to be included in the study domain, we classify their drought condition during all of those months, following Svoboda et al. (37) as shown in *SI Appendix*, Table S1. During months where the conditions are not met (i.e., either less than 75% of the values are nonzero or the 3-mo climatological MODIS SC value for a grid box is less than 5%), we assign that grid box a near-normal (NN) designation across all years. We use this classification for grid boxes that have values close to climatology or do not meet the above SWE and SC criteria to be robustly classified using *SI Appendix*, Table S1, during all months of the year. The latter type of assignment is only applied for mapping. We exclude those grid boxes from our distributional analysis when NN is assigned for this reason.

Since we use a general drought monitoring framework, it can be applied to other SWE datasets in the future when higher-resolution global snow data become available. Analysis can also be performed at the regional scale. Although our approach has the flexibility to be applied at different time scales, longer time scales (e.g., 6, 12, 24, and 48 mo) do not carry the same meaning as for other drought-related variables (soil moisture and precipitation) since a region with a seasonal snowpack commonly has several consecutive months of no SWE (e.g., complete melt out during the summer). Moreover, it is also possible to use a shorter time scale (e.g., 1 mo) for drought analysis; however, a short time scale can be more sensitive to the occurrence of a single event (snowstorm or melt event), particularly near the beginning of the accumulation season or during the melt season. We therefore use a 3-mo time scale throughout this study. We also restrict snow drought duration analysis to a maximum length of 6 mo for this same reason (November to April in the Northern Hemisphere and May to October in the Southern Hemisphere) even though a drought may be observed during multiple consecutive snow seasons.

Verification. To verify the timing and spatial coherence of the snow drought patterns observed using our SWEI method, we do not use ground-based in situ observations (i.e., snow courses and snow pillows) because of the large spatial disparity between a point-scale measurement and the grid-averaged MERRA-2 dataset. Instead, we compare our results with SWE anomalies computed using other available gridded SWE estimates over the contiguous United States (CONUS) and Afghanistan, using SWE from SNODAS and FEWS NET, respectively (61). Selected examples for these regions correspond to case studies presented in Figs. 2 and 3.

Our verification of the MERRA-2 SWEI (*SI Appendix*, Figs. S1 and S2) focuses on understanding consistency in terms of general temporal and spatial patterns of wet and dry cycling given differences in reference data type and resolutions. Although SNODAS and FEWS NET yield 1-km SWE information, they provide regionally specific products with record lengths <20 y, whereas MERRA-2 is a nearly 40-y global dataset. While a remote sensing-based SWE dataset such as GlobSnow (67) also provides SWE estimates over the Northern Hemisphere, GlobSnow does not yield SWE values over mountainous regions (such as those in the WUS or Afghanistan study domains).

SI Appendix, Figs. S1 and S2, each indicate that MERRA-2 is capable of monitoring wet and dry cycles as the SWEI maps show consistency among the temporal and spatial patterns exhibited by the other datasets. *SI Appendix*, Fig. S1 *A* and *B*, shows dry regions in the WUS, a wet band to the east of that region, and dry midwestern and wet northeastern states. Similarly, spatial coherence of wet and dry cycles and their patterns are observed in *SI Appendix*, Fig. S1 *C* and *D*, with wet conditions developing and persisting in the WUS, while drought conditions emerge at the intersection of the midwestern, southern, and northeastern regions of the United States. In *SI Appendix*, Fig. S2, the majority of Afghanistan and countries along its northeastern boundary display strong drought conditions. Small, fine-scale regions with above-average SWE, as identified by FEWS NET in column 1, are however not resolved by MERRA-2 (column 2) since a higher-resolution dataset is necessary to capture such heterogeneities. Nonetheless, *SI Appendix*, Figs. S1 and S2, demonstrate overall consistencies and spatial coherence between the MERRA-2 SWEI and anomalies from the other datasets.

Despite the verification of our SWEI approach in *SI Appendix*, Figs. S1 and S2, additional validations and agency partnerships are needed before our snow drought monitoring can be implemented operationally. The following section describes some additional limitations associated with our study.

Limitations. In this study, we utilize MERRA-2 SWE to understand and characterize snow droughts across the globe. We acknowledge that the spatial resolution of MERRA-2 limits our ability to capture the high heterogeneity of SWE that occurs in complex mountainous terrain. Construction of a high-resolution global SWE dataset has not yet been achieved. Given limited availability of SWE observations and information across the globe, large uncertainties in precipitation and SWE estimates can occur, especially in high mountain Asia where ∼800 million people depend on snow and ice melt and face food insecurity issues (20, 68).

As noted above, we consider SWE at 3-mo time scales, which is commonly used in drought assessments and accounts for both the magnitude of the accumulated SWE and its persistence. This differs from previous SWE-related studies that investigate trends in maximum snow (SWE or snow depth) accumulation (i.e., peak SWE or SWE on a set date such as 1 April in the western United States). Since our drought assessment considers changes in the snowpack at 3-mo time scales, the patterns or distributional changes observed herein may not match those found in studies focusing on the maximum SWE or a different (e.g., monthly) time scale.

Data Availability. Data supporting the conclusions of this study can be obtained from https://doi.org/10.6084/m9.figshare.c.5055179. MERRA-2 data are available from https://gmao.gsfc.nasa.gov/reanalysis/MERRA-2/data_access/. MODIS/Terra monthly snow cover data are available from https://doi.org/10.5067/MODIS/MOD10CM.006. The SNODAS and FEWS NET SWE information used in *SI Appendix* over CONUS and Afghanistan can be downloaded from https://doi.org/10.7265/N5TB14TC and https://earlywarning.usgs.gov/fews/product/188, respectively.

ACKNOWLEDGMENTS. This work was partially supported by the National Science Foundation (NSF) Earth Sciences Postdoctoral Fellowship Award EAR-1725789, NSF Award OAC-1931335, National Aeronautics and Space Administration (NASA) Grant NNX16AO56G, and National Oceanic and Atmospheric Administration (NOAA) Grant NA14OAR4310222.

1. T. P. Barnett, J. C. Adam, D. P. Lettenmaier, Potential impacts of a warming climate on water availability in snow-dominated regions. *Nature* **438**, 303–309 (2005).
2. R. C. Bales *et al*., Mountain hydrology of the western United States. *Water Resour. Res.* **42**, W08432 (2006).
3. A. L. Westerling, H. G. Hidalgo, D. R. Cayan, T. W. Swetnam, Warming and earlier spring increase western U.S. forest wildfire activity. *Science* **313**, 940–943 (2006).
4. T. W. Estilow, A. H. Young, D. A. Robinson, A long-term Northern Hemisphere snow cover extent data record for climate studies and monitoring. *Earth Syst. Sci. Data* **7**, 137–142 (2015).
5. D. K. Hall, A. Frei, S. J. Déry, "Remote sensing of snow extent" in *Remote Sensing of the Cryosphere*, M. Tedesco, Ed. (Wiley Blackwell, 2015), pp. 31–47.
6. D. K. Hall, G. A. Riggs, V. V. Salomonson, N. E. DiGirolamo, K. J. Bayr, MODIS snow-cover products. *Remote Sens. Environ.* **83**, 181–194 (2002).
7. A. Frei, D. A. Robinson, Northern Hemisphere snow extent: Regional variability 1972-1994. *Int. J. Climatol.* **19**, 1535–1560 (1999).
8. N. C. Grody, A. N. Basist, Global identification of snowcover using SSM/I measurements. *IEEE Trans. Geosci. Remote Sens.* **34**, 237–249 (1996).
9. J. J. Simpson, J. R. Stitt, M. Sienko, Improved estimates of the areal extent of snow cover from AVHRR data. *J. Hydrol.* **204**, 1–23 (1998).
10. R. L. Armstrong, M. J. Brodzik, Recent northern hemisphere snow extent: A comparison of data derived from visible and microwave satellite sensors. *Geophys. Res. Lett.* **28**, 3673–3676 (2001).
11. D. K. Hall, G. A. Riggs, Accuracy assessment of the MODIS snow products. *Hydrol. Processes* **21**, 1534–1547 (2007).
12. J. C. Hammond, F. A. Saavedra, S. K. Kampf, Global snow zone maps and trends in snow persistence 2001-2016. *Int. J. Climatol.* **38**, 4369–4383 (2018).
13. J. Dozier, E. H. Bair, R. E. Davis, Estimating the spatial distribution of snow water equivalent in the world's mountains. *WIREs. Water* **3**, 461–474 (2016).
14. D. P. Lettenmaier *et al*., Inroads of remote sensing into hydrologic science during the WRR era. *Water Resour. Res.* **51**, 7309–7342 (2015).
15. T. H. Painter *et al*., The Airborne Snow Observatory: Fusion of scanning lidar, imaging spectrometer, and physically-based modeling for mapping snow water equivalent and snow albedo. *Remote Sens. Environ.* **184**, 139–152 (2016).
16. M. Tedesco, C. Derksen, J. S. Deems, J. L. Foster, "Remote sensing of snow depth and snow water equivalent" in *Remote Sensing of the Cryosphere*, M. Tedesco, Ed. (Wiley Blackwell, 2015), pp. 73–98.
17. A. W. Nolin, Recent advances in remote sensing of seasonal snow. *J. Glaciol.* **56**, 1141–1150 (2010).
18. P. W. Mote, S. Li, D. P. Lettenmaier, M. Xiao, R. Engel, Dramatic declines in snowpack in the western US. *npj Clim. Atmos. Sci.* **1**, 2 (2018).
19. L. S. Huning, A. AghaKouchak, Mountain snowpack response to different levels of warming. *Proc. Natl. Acad. Sci. U.S.A.* **115**, 10932–10937 (2018).
20. W. W. Immerzeel, L. P. H. van Beek, M. F. P. Bierkens, Climate change will affect the Asian water towers. *Science* **328**, 1382–1385 (2010).
21. A. Fontrodona Bach, G. Schrier, L. A. Melsen, A. M. G. Klein Tank, A. J. Teuling, Widespread and accelerated decrease of observed mean and extreme snow depth over Europe. *Geophys. Res. Lett.* **45**, 12312–12319 (2018).
22. T. Smith, B. Bookhagen, Changes in seasonal snow water equivalent distribution in High Mountain Asia (1987 to 2009). *Sci. Adv.* **4**, e1701550 (2018).
23. P. W. Mote, A. F. Hamlet, M. P. Clark, D. P. Lettenmaier, Declining mountain snowpack in western North American. *Bull. Am. Meteorol. Soc.* **86**, 39–50 (2005).
24. M. Staudinger, K. Stahl, J. Seibert, A drought index accounting for snow. *Water Resour. Res.* **50**, 7861–7872 (2014).
25. B. A. Shafer, L. E. Dezman, "Development of a surface water supply index (SWSI) to assess the severity of drought conditions in snowpack runoff areas" in *Proceedings of the Western Snow Conference*, (Western Snow Conference, 1982), pp. 164–175.
26. A. Muhammad, S. Kumar Jha, P. F. Rasmussen, Drought characterization for a snow-dominated region of Afghanistan. *J. Hydrol. Eng.* **22**, 5017014 (2017).
27. B. J. Hatchett, D. J. McEvoy, Exploring the origins of snow drought in the northern Sierra Nevada, California. *Earth Interact.* **22**, 1–13 (2018).
28. J. R. Dierauer, D. M. Allen, P. H. Whitfield, Snow drought risk and susceptibility in the western United States and southwestern Canada. *Water Resour. Res.* **55**, 3076–3091 (2019).
29. S. A. Margulis *et al*., Characterizing the extreme 2015 snowpack deficit in the Sierra Nevada (USA) and the implications for drought recovery. *Geophys. Res. Lett.* **43**, 6341–6349 (2016).
30. B. Zhang *et al*., A framework for global multicategory and multiscalar drought characterization accounting for snow processes. *Water Resour. Res.* **55**, 9258–9278 (2019).
31. A. Harpold, M. Dettinger, S. Rajagopal, Defining snow drought and why it matters. *Eos*, 98, 10.1029/2017EO068775 (2017).
32. S. A. Margulis, G. Cortés, M. Girotto, M. Durand, A Landsat-era Sierra Nevada snow reanalysis (1985–2015). *J. Hydrometeorol.* **17**, 1203–1221 (2016).
33. L. S. Huning, A. AghaKouchak, Global snow drought data set. Figshare. https://doi.org/10.6084/m9.figshare.c.5055179. Deposited 9 July 2020.
34. R. Gelaro *et al*., The Modern-Era Retrospective Analysis for Research and Applications, version 2 (MERRA-2). *J. Clim.* **30**, 5419–5454 (2017).
35. M. J. Hayes, C. Alvord, J. Lowry, Drought indices. *Intermountain West Clim. Summ.* **3**, 2–6 (2007).
36. World Meteorological Organization, Global Water Partnership, Handbook of Drought Indicators and Indices. https://www.droughtmanagement.info/handbook-drought-indicators-and-indices/ (2016). Accessed 5 July 2018.
37. M. Svoboda *et al*., The drought monitor. *Bull. Am. Meteorol. Soc.* **83**, 1181–1190 (2002).
38. J. L. Cohen, J. C. Furtado, M. A. Barlow, V. A. Alexeev, J. E. Cherry, Arctic warming, increasing snow cover and widespread boreal winter cooling. *Environ. Res. Lett.* **7**, 14007 (2012).
39. J. Zhang, W. Tian, M. P. Chipperfield, F. Xie, J. Huang, Persistent shift of the Arctic polar vortex towards the Eurasian continent in recent decades. *Nat. Clim. Chang.* **6**, 1094–1099 (2016).
40. I. Cvijanovic *et al*., Future loss of Arctic sea-ice cover could drive a substantial decrease in California's rainfall. *Nat. Commun.* **8**, 1947 (2017).
41. P. W. Mote *et al*., Perspectives on the causes of exceptionally low 2015 snowpack in the western United States. *Geophys. Res. Lett.* **43**, 10980–10988 (2016).
42. M. G. Cooper, A. W. Nolin, M. Safeeq, Testing the recent snow drought as an analog for climate warming sensitivity of Cascades snowpacks. *Environ. Res. Lett.* **11**, 84009 (2016).
43. M. E. Marlier *et al*., The 2015 drought in Washington State: A harbinger of things to come? *Environ. Res. Lett.* **12**, 114008 (2017).
44. S. Belmecheri, F. Babst, E. R. Wahl, D. W. Stahle, V. Trouet, Multi-century evaluation of Sierra Nevada snowpack. *Nat. Clim. Chang.* **6**, 2–3 (2016).
45. R. Howitt, D. MacEwan, J. Medellín-Azuara, J. Lund, D. Sumner, "Economic analysis of the 2015 drought for California agriculture" (Center for Watershed Sciences, University of California, Davis, 2015), p. 31.
46. E. H. Bair, A. Abreu Calfa, K. Rittger, J. Dozier, Using machine learning for real-time estimates of snow water equivalent in the watersheds of Afghanistan. *Cryosphere* **12**, 1579–1594 (2018).
47. International Federation of Red Cross and Red Crescent Societies, Emergency Plan of Action (EPoA) Afghanistan: Drought 2018. https://reliefweb.int/report/afghanistan/afghanistan-drought-emergency-plan-action-epoa-dref-n-mdraf004 (2018). Accessed 25 July 2019.
48. Food and Agriculture Organization of the United Nations, Farmers grappling with Afghanistan drought urgently need seed and animal feed support. http://www.fao.org/news/story/en/item/1171752/icode/ (2018). Accessed 4 June 2019.
49. C. P. Kelley, S. Mohtadi, M. A. Cane, R. Seager, Y. Kushnir, Climate change in the Fertile Crescent and implications of the recent Syrian drought. *Proc. Natl. Acad. Sci. U.S.A.* **112**, 3241–3246 (2015).
50. N. P. Evans *et al*., Quantification of drought during the collapse of the classic Maya civilization. *Science* **361**, 498–501 (2018).
51. M. Zemp *et al*., Global glacier mass changes and their contributions to sea-level rise from 1961 to 2016. *Nature* **568**, 382–386 (2019).
52. B. Nandintsetseg, M. Shinoda, B. Erdenetsetseg, Contributions of multiple climate hazards and overgrazing to the 2009/2010 winter disaster in Mongolia. *Nat. Hazards* **92**, 109–126 (2018).
53. International Federation of Red Cross and Red Crescent Societies, Emergency appeal operations update Mongolia: Extreme winter condition. https://reliefweb.int/report/mongolia/mongolia-extreme-winter-condition-mdrmn005-emergency-appeal-operations-update-n-1. Accessed 22 June 2019.
54. M. Huss *et al*., Toward mountains without permanent snow and ice. *Earths Future* **5**, 418–435 (2017).
55. Y. Qin *et al*., Agricultural risks from changing snowmelt. *Nat. Clim. Chang.* **10**, 459–465 (2020).
56. R. H. Reichle *et al*., Assessment of MERRA-2 land surface hydrology estimates. *J. Clim.* **30**, 2937–2960 (2017).
57. P. D. Broxton, X. Zeng, N. Dawson, Why do global reanalyses and land data assimilation products underestimate snow water equivalent? *J. Hydrometeorol.* **17**, 2743–2761 (2016).
58. M. L. Wrzesien, M. T. Durand, T. M. Pavelsky, A reassessment of North American river basin cool-season precipitation: Developments from a new mountain climatology data set. *Water Resour. Res.* **55**, 3502–3519 (2019).
59. T. Carroll *et al*., "NOHRSC Operations and the simulation of snow cover properties for the coterminous U.S." in *Proceedings of the 69th Annual Meeting of the Western Snow Conference*, (Western Snow Conference, 2001), p. 14.
60. National Operational Hydrologic Remote Sensing Center, *Snow Data Assimilation System (SNODAS) Data Products at NSIDC, Version 1*, (National Snow and Ice Data Center, 2004), https://doi.org/10.7265/N5TB14TC.
61. Famine Early Warning System Network, Snow Water Equivalent Anomaly with Provinces. (Famine Early Warning System Network) https://earlywarning.usgs.gov/fews/product/188. Accessed 25 July 2019.
62. D. K. Hall, G. A. Riggs, *MODIS/Terra Snow Cover Monthly L3 Global 0.05Deg CMG, Version 6*, (NASA National Snow and Ice Data Center Distributed Active Archive Center, 2015), https://doi.org/10.5067/MODIS/MOD10CM.006.
63. D. S. Wilks, *Statistical Methods in the Atmospheric Sciences*, (Academic Press, ed. 2, 2006).
64. A. Farahmand, A. AghaKouchak, A generalized framework for deriving nonparametric standardized drought indicators. *Adv. Water Resour.* **76**, 140–145 (2015).
65. I. I. Gringorten, A plotting rule for extreme probability paper. *J. Geophys. Res.* **68**, 813–814 (1963).
66. A. AghaKouchak, A baseline probabilistic drought forecasting framework using standardized soil moisture index: Application to the 2012 United States drought. *Hydrol. Earth Syst. Sci.* **18**, 2485–2492 (2014).
67. M. Takala *et al*., Estimating northern hemisphere snow water equivalent for climate research through assimilation of space-borne radiometer data and ground-based measurements. *Remote Sens. Environ.* **115**, 3517–3529 (2011).
68. H. D. Pritchard, Asia's shrinking glaciers protect large populations from drought stress. *Nature* **569**, 649–654 (2019).